Articles in PresS. Am J Physiol Renal Physiol (May 10, 2017). doi:10.1152/ajprenal.00428.2016

IL-6 promotes epithelial-to-mesenchymal transition of human peritoneal mesothelial cells possibly through JAK2/STAT3 signaling pathway

Jing Xiao[1]，Yanan Gong[1], Ying Chen[1,2], Dahai Yu[1,2], Xiaoyang Wang[1], Xiaoxue Zhang[1], Yanna Dou[1], Dong Liu[1], Genyang Cheng[1], Shan Lu[1], Wenming Yuan[1], Yansheng Li[1], and Zhanzheng Zhao[1]*

[1]The Nephrology Centre of the First Affiliated Hospital of Zhengzhou University, 1 Jianshe Eastern Road, Erqi District, Zhengzhou 450052, Henan, China

[2]Arthritis Research UK Primary Care Centre, Research Institute for Primary Care & Health Sciences, Keele University, Keele ST5 5BG, UK

Corresponding author:

Zhanzheng Zhao,

Department of Nephrology,

The First Affiliated Hospital of Zhengzhou University,

Nephropathy Research Institutes of Zhengzhou University,

1 Jianshedong Road Erqi District

Zhengzhou 450052,

China

Tel: +86 371 66295962

Fax: +86 371 66295964

E-mail: zzzdoctor@139.com

Copyright © 2017 by the American Physiological Society.

Abstract

Long-term peritoneal dialysis (PD) therapy results in functional and structural alteration of the peritoneal membrane, including epithelial-to-mesenchymal transition (EMT). Interleukin 6 (IL-6) is a local pleiotropic cytokine, hypothesized to play an important role in EMT. This study was designed to investigate the role of IL-6 in EMT and peritoneal membrane dysfunction in long-term PD patients by assessing the level of IL-6 in dialysate and exploring the relationship between IL-6, the related signaling pathway JAK2/STAT3, and EMT, using in vitro cellular and molecular techniques. Plasma and dialysate levels of IL-6 were significantly higher in PD ultrafiltration failure patients compared to those in patients without ultrafiltration failure and were negatively correlated with measures of PD adequacy. In vitro, IL-6 treatment changed human peritoneal mesothelial cell phenotype from a typical cobblestone-like to a fibroblast-like appearance and increased cell viability. IL-6 treatment increased α-SMA and VEGF expression but decreased E-cadherin expression. IL-6 treatment activated the JAK/STAT signaling pathway. However, the JAK2/STAT3 inhibitor WP1066 prevented IL-6-induced activation of the JAK2/STAT3 pathway and EMT. We conclude that IL-6 promotes the EMT process, possibly by activating the JAK2/STAT3 signaling pathway. IL-6 may serve as a novel therapeutic target for preventing EMT, and preservation of the peritoneal membrane may arise from these studies.

Keywords: Peritoneal dialysis, interleukin 6, epithelial-to-mesenchymal transition, human peritoneal mesothelial cells, JAK2/STAT3, WP1066,

Introduction

Peritoneal dialysis (PD) has drawn increasing attention as a common therapeutic method for end-stage renal disease (ESRD) other than hemodialysis and renal transplantation. However, long-term PD therapy is known to result in functional and structural alterations in the peritoneal membrane (7). Peritoneal pathology can be induced by several stresses inherent in PD therapy, for example exposure of the peritoneal membrane to PD fluid, catheter trauma, and peritonitis (26).

Interleukin 6 (IL-6) is a pleiotropic cytokine that plays an important role in multiple pathological and physiological processes. It was found that increased circulating level of IL-6 predicted poor outcome in patients with haemodialysis and PD (21). In a model of acute peritoneal inflammation, fibrosis was strictly dependent on IL-6 via IL-6-mediated T helper 1 cell effector commitment and the emergence of STAT1 (signal transducer and activator of transcription-1) activity within the peritoneal membrane (8). It was observed that IL-6 levels were higher in drained dialysate than in the circulation, suggesting that the peritoneal membrane produces local IL-6 during PD (19).

The epithelial-to-mesenchymal transition (EMT) is a process by which epithelial cells lose their cell polarity and cell-cell adhesion and gain migratory and invasive properties to become mesenchymal stem cells. EMT is essential for numerous physiological and pathological processes including wound healing (31), fibrogenic diseases (e.g. peritoneal fibrosis, glomerular fibrosis), and renal dysfunction in diabetic nephropathy (1，11). Several biomarkers for EMT have been identified, such as the loss of the E-cadherin (an epithelial adhesion protein), the upregulation of the α-smooth muscle actin (α-SMA, a mesenchymal marker) and the upregulation of the vascular endothelial growth factor (VEGF, a signalling protein involved in both vasculogenesis and angiogenesis) (34).

The Janus Kinase/Signal Transducer and Activator of Transcription (JAK/STAT) pathway is a pleiotropic cascade essential to signal transduction of cytokines

from the cell membrane to the nucleus. It has been reported to mediate various cellular functions, including gene activation and cell proliferation, differentiation and apoptosis (6). JAK/STAT pathway contributed importantly to synthesis of extracellular matrix proteins (29). The analysis of glomeruli and tubulointerstitium in kidney biopsies in diabetic nephropathy patients exhibited increased expression of JAK/STAT pathway (2).

IL-6 was associated with increased expression of several pro-fibrotic (18) and pro-inflammatory genes (25), and was found as a promoter of the JAK/STAT pathway (14). Recent study showed that IL-6 can specifically activate STAT3 via its corresponding receptor (IL-6R), and therefore can lead to activation of the JAK/STAT signaling pathway (30). In the research area of PD care, despite the evidence of EMT of peritoneal mesothelial cells in patients undergoing PD, few studies exist on the relationship between IL-6, the related signaling pathway (JAK2/STAT3) and the EMT.

The objective of the current study therefore was to investigate the relationship between IL-6 and peritoneal membrane injury and the possible mechanism of IL-6-induced EMT through the JAK2/STAT3 signaling pathway. WP1066, an inhibitor of JAK2/STAT3, was used to investigate the role of JAK2/STAT3 in the process of EMT.

Materials and methods

Clinical epidemiology

Patients

A cohort consisted of 40 ESRD patients between 1st of September 2015 and 31st August 2016 were recruited, from the Nephrology Centre of the First Affiliated Hospital of Zhengzhou University, Henan, China. The study was approved by the Ethics Committee of Zhengzhou University. Written informed consent was obtained from all patients before enrollment.

Patient recruitment criteria are shown in Table 1. Patients were separated into 2 groups [ultrafiltration failure (UFF) and adequate UF], according to the International Society for PD guidelines (16), which are based on peritoneal equilibration test (PET) for volume and small solute clearance. After 2000 ml of 4.25% dextrose-containing dialysate is left in the peritoneal cavity for 4 hours,

less than 400 ml of UF indicates UFF, and dialysate/plasma creatinine ratio (D/PCr) of more than 0.7 is consistent with the rapid small molecule transport status often seen in UFF. Patient data included demographic-clinical [age, gender, BMI, body surface area (BSA), PD duration], laboratory (serum albumin, Hs-CRP, hemoglobin) and PD adequacy measures (total Kt/v urea, peritoneal Kt/v urea, renal Kt/v urea, urine output, 24 hours ultrafiltration, dialysate glucose exposure), the peritoneal equilibration test (PET) (4 hours ultrafiltration, D/PCr), and the plasma and dialysate IL-6 levels .

IL-6 level

ELISA was used to measure the level of IL-6 in collected plasma and peritoneal dialysate fluid (PDF) samples according to manufacturer's instructions (CSB-E04638h, CUSABIO, Wuhan, China). Plasma was taken during peritoneal equilibration test and immediately frozen at −80°C until analysis. PDF was collected after overnight dwell (8-10 hours) before stored in at -80°C. Samples were thawed once only during the aliquoting process prior to analysis. Each sample was examined in duplicate. A Bio-Rad well-reader (iMark, Bio-Rad, Hercules, CA, USA) was used with the absorbance at 450 nm. Since the dialysate IL-6 level was influenced by ultrafiltration volume, it was assessed as IL-6AR (IL-6 Appearance rate), calculated by dialysate concentration×drained volume/dwell time (pg/min).

Cellular and molecular *biology*

Cell

HPMCs were obtained Professor Pierre Ronco (TENON, Paris, France). Cells were routinely cultured in Dulbecco's modified Eagle's medium (DMEM, HyClone, Logan, Utah) supplemented with 10% fetal bovine serum (FBS, Bioland, San Diego, California, United States), 100 UI/mL penicillin and 100 μg/mL streptomycin. Recombinant human IL-6 (Peprotech, New Jersey, United States) was dissolved in DMEM.

MTT assay

3-(4,5-Dimethylthiazol-2-yl)-2,5-diphenyltetrazolium bromide (MTT) (Sigma, St. Louis, MO, USA) was used. HPMCs were seeded into a 96-well plate (approximately 4,000 cells per well) and cultured to 40%–50% confluence.

Twenty μL of MTT (5 mg/mL) was added to each well before further incubated for another 4 hours. Subsequently, 100 μL of dimethyl sulfoxide (DMSO) was added to each well and mixed thoroughly, after culture medium was discarded. Wells were then read at 490 nm using a microplate reader (iMark, Bio-Rad, Hercules, CA, USA).

Western blotting

Protein from HPMCs was homogenized in lysis buffer and was quantified. Each protein sample (30 μg) was separated by 10% SDS-PAGE and transferred onto a nitrocellulose membrane. At 4°C, the membrane was simultaneously exposed overnight to mouse anti-α-SMA monoclonal antibody (Wuhan Boster Biological Technology Ltd., Wuhan, China) in a 1:500 dilution, to rabbit polyclonal anti-E-cadherin antibody, rabbit polyclonal anti-VEGF antibody, rabbit polyclonal anti-JAK2 antibody (Proteintech, Manchester, UK) and rabbit polyclonal anti-phospho-JAK2 antibody (Beijing Biosynthesis Biotechnology Co. LTD., Beijing, China) in a 1:1000 dilution, to rabbit monoclonal anti-phosphor-STAT3 (S727) antibody (Abcam, Cambridge, MA, USA) and rabbit polyclonal anti-STAT3 antibody (Proteintech, Manchester, UK) in a 1:5000 dilution, and to mouse monoclonal anti-β-actin antibody (Wuhan Boster Biological Technology Ltd., Wuhan, China) a 1:4000 dilution. After rinsing with 1×TBS, 0.1% Tween-20 solution four times every 5 minutes, each membrane was incubated with horseradish peroxidase-conjugated secondary antibody, goat anti-rabbit IgG or goat anti-mouse IgG (1:10,000 in dilution, Proteintech, Manchester, UK) for 1 hour at room temperature. After another wash with 1×TBS, 0.1% Tween-20 solution four times every 5 minutes, data were analysed using an enhanced chemiluminescence Western blot detection system (FluorChem E, proteinsimple, USA).

RNA extraction and quantitative real-time PCR

Total cellular RNA was extracted using RNAiso Plus (Takara Bio, Inc., Shiga, Japan), and contaminating DNA was removed using RNAase-free DNase. The DNA-free RNA was reverse-transcribed into cDNA using the RevertAid First Stand cDNA Synthesis Kit (Thermo Fisher Scientific Inc., Massachusetts, United States). Real-time fluorescence quantitative PCR was performed on the 7500 Fast Real-Time PCR system using SYBR Green as double-stranded DNA-specific dye in accordance with the manufacturer's instructions (Life Technologies, Thermo Fisher Scientific, MA, USA). All primers used in the

PCR were designed using the Primer Express 2.0 software (Applied Biosystems) and checked for homology using BLAST (see Table 2). The relative mRNA expression level of the target genes in each sample were calculated using the $2^{-\Delta\Delta CT}$ method.

WP1066

WP1066 (Selleck Chemicals LLC, USA) is an effective STAT3 pathway inhibitor (23,27), a small molecule that can selectively block the phosphorylation of JAK2 and STAT3.

Statistical analysis

Data (continues variable) were expressed as mean with standard deviation (SD) or median with interquartile range (IQR) dependent on the data distribution. Comparison between two groups was analysed using Student's T or Mann Whitney test dependent on the data distribution. Pearson's correlation test was used to assess possible correlation. A p-value < 0.05, two tailed, was considered as statistical significance. All statistical analysis was carried out in SPSS version 17.0.

Results

Clinical epidemiology

Level of IL-6 in plasma and dialysate in ESRD cohort

Patient demographic and clinical characteristics, and particularly plasma and dialysate IL-6 levels, stratified by PD/UFF status, are shown in Table 3. The mean age of the cohort was 42 years, with 18 (45%) females. Not surprisingly, characteristics demonstrating PD adequacy were different in PD patients without UFF compared to those with UFF. However, no difference in other patient characteristics was seen between the two subsets. IL-6 levels (both in dialysate and plasma) were higher in UFF patients, compared to those in patients with PD care.

Table 4 shows the correlation between IL-6 level in dialysate and the selected patient characteristics. Level of IL-6 in dialysate was positively associated with PD duration ($r = 0.39$) and D/PCr ($r = 0.63$) but negatively correlated with

measures of PD adequacy in relatively strong relationships ($r > 0.3$) in all patients.

Cellular and molecular *biology*

Effect of IL-6 on cell morphology and viability

Morphologic change of HPMCs occurred when cells were continuously stimulated by IL-6 at a level of 50 ng/mL or higher for 5 days, with an apparent dose-response effect. HPMCs converted into fibroblast-like appearance, from the initial cobblestone-like cell (see Figure 1A). HPMCs showed an increased cell proliferation with IL-6 stimulation (50 ng/mL, for 24 hours or longer), compared to those not exposed to IL-6 but cultured in the same condition (see Figure 1B).

Effect of IL-6 on EMT related proteins in HPMC

α-SMA and VEGF was significantly increased whereas E-cadherin was downregulated with regard to the protein and mRNA expressions in IL-6 stimulated HPMCs at 24 hours (see Figure 2A-B for protein data and 2C-E for mRNA data), with an apparent dose effect (none vs. 50 ng/mL vs. 100 ng/mL IL-6). Data also showed that the stimulatory effects were time-dependent up through the 24 hours tested (see Figure 3).

Effect of IL-6 on JAK2/STAT3 signaling pathway in HPMC

No difference in the total protein expressions of JAK2 and STAT3 was observed before and after IL-6 treatment. However, the phosphorylated protein of JAK2 and STAT3 were significantly increased (see Figure 4 A,C). Data also showed that the activation effects were dose-dependent (Figure 4 A,B) and time-dependent (Figure 4 C,D).

Effect of WP1066 on JAK2/STAT3 pathway and EMT process

P-STAT/STAT3 expression decreased significantly after treatment with 10 *μM* WP1066 for 24 hours (Figure 5), confirming that WP1066 was a JAK2/STAT3 inhibitor in our cell system. Therefore, 10 *μM* WP1066 was used in the experiments for preventing the JAK2/STAT3 signaling pathway. Figure 6

shows that treatment of HPMC with 10 *μM* WP1066 alone for 24 hours did not alter phosphorylation of JAK and STAT or total JAK and STAT expression, compared to untreated cells. However, WP1066 prevented IL-6 from increasing phosphorylation of JAK and STAT.

Addition of WP1066 eliminated the effect of IL-6 on α-SMA, VEGF and E-cadherin (see Figure 7) and therefore prevented the EMT process.

Effect of WP1066 on cell morphology and viability

Morphologic change of HPMCs occurred when cells were continuously stimulated by IL-6 at a level of 50 ng/mL for 5 days. When adding WP1066, the effect of IL-6 was prevented (see Figure 8A). HPMCs showed an increased cell proliferation with IL-6 stimulation (50 ng/mL, 24 hours), compared to those without but cultured in the same condition. But this increasing cell viability was prevented by WP1066 (see Figure 8B).

Discussion

PD and hemodialysis are well-established treatments for patients with ESRD. PD has several advantages compared with hemodialysis, including a simpler and less invasive procedure and the retention of residual renal function (3,4). The peritoneum is a membrane with good penetration ability. PD clears metabolic waste products and toxins and corrects water, electrolyte, and acid-base disorders, using diffusion, ultrafiltration, and absorption. Peritoneal ultrafiltration is affected by several factors such as transmembrane pressure gradient, effective peritoneal surface area and aquaporin function (32). Continuous exposure to conventional PD solutions contributes to progressive peritoneal injury, which is an important source of local inflammation that can result in adverse functional outcome such as higher peritoneal solute transport rate (PSTR). Higher PSTR is a widely accepted risk factor for mortality and technique failure in PD patients (24).

The IL-6 system (both dialysate and systemic) has been found to be associated with variability in PSTR (13, 20). In our study, the levels of IL-6 (either plasma of dialysate) in patients with UFF were significantly higher than those in patients without UFF. Furthermore, the dialysate level of IL-6 was found to be correlated positively with PD duration and D/PCr, and negatively

with total Kt/v urea, peritoneal Kt/v urea, urine output, 24 hours ultrafiltration and 4 hours ultrafiltration, suggesting that the dialysate IL-6 level is an indicator of peritoneal UFF. Our results are in line with those from a previous study which also showed that increased dialysate IL-6 level was associated with more years doing PD therapy, and was a predictor of PSTR (5).

A recent study demonstrated that long-term overexpression of IL-6 might promote fibrosis by regulating pro-fibrotic T-cell populations (8). In the mouse model of peritoneal fibrosis, transfer of helper T cell type 1 effector T cell secreting interferon-γ (IFN- γ) (under IL-6/STAT1 control) restored progression to fibrosis in IL-6 knockout mouse by altering the normal control by metalloproteinases of extracellular matrix turnover (8). In our study, HPMCs treated with IL-6 showed morphological change towards fibroblast-like cells, suggesting that the presence of overexpressed IL-6 may promote fibrosis in peritoneal membrane.

The JAK2/STAT3 signaling pathway affects various basic cell functions in response to extra-cellular cytokines and growth factors, such as cell growth, differentiation and death (28). In association with the above classical pathway, recently the signaling loop of IL-6/ glycoprotein 130 (gp130)/STAT3 was shown to play a crucial role in the pathogenesis of lung fibrosis (17). In another study the IL-6/Stat3/Akt signaling axis played a protective role in type 2 pneumocytes by regulating surfactant homeostasis (22). In the mouse model of $gp130^{F/F}$, IL-6 trans-signaling via STAT3 is a critical modulator of the lipopolysaccharide (LPS)-driven pro-inflammatory response through cross-talk regulation of the TLR4/Mal signaling pathway (9). IL-6 administration *in vitro* promoted STAT3 activity and collagen I expression and this study suggested the multiple roles of IL-6 in renal fibrosis (33).

There were many proposed pathways associated with the pathogenesis of peritoneal fibrosis during PD treatment such as the endothelial nitric oxide synthase (eNOS)-NO signaling pathway (12), Serum response factor (SRF) signaling (10), the phosphatidylinositol 3-kinase (PI3K)/AKT (also known as PKB or protein kinase B) signaling pathway (15). However, the specific involvement of IL-6 in peritoneal fibrosis is poorly understood. In our study, data showed that the phosphorylation of JAK2 and STAT3 in HPMCs were significantly increased in response to the treatment of IL-6, implying that IL-6

may be able to active JAK2/STAT3 signaling in vitro. The current study was the first to investigate the possible effect of IL-6 on the JAK2/STATA3 in peritoneal fibrosis. Although the mechanism is still largely unknown, our results at both the clinical and cellular/molecular levels suggest that IL-6 may be an important pro-EMT cytokine in PD therapy. This study provides initial and important insights into the mechanisms of IL-6 in the EMT process of HPMCs and may lead to therapeutic strategies to slow peritoneal fibrosis.

ACKNOWLEDGMENTS

The authors thank Professor Pierre Ronco (TENON, Paris, France) for providing HPMCs cells. The authors thank Professor Guoqiang Zhao and Basic Research Centre, Academy of Medical Science, Zhengzhou University for excellent technical assistance. This work was supported by the National Nature Science Foundation of China (grant 340600531870).

DISCLOSURES

No conflicts of interest, financial or otherwise, are declared by the author(s).

AUTHOR CONTRIBUTIONS

Jing Xiao，Yanan Gong, Xiaoyang Wang, Xiaoxue Zhang and Yanna Dou performed experiments; Yanan Gong, Ying Chen and Dahai Yu carried out statistical analysis. Shan Lu, Wenming Yuan and Yansheng Li interpreted results of experiments; Jing Xiao and Yanan Gong drafted manuscript; Ying Chen, Dahai Yu, Dong Liu and Genyang Cheng edited and revised manuscript; Zhanzheng Zhao designed the study and approved final version of manuscript.

REFERENCE

1. **Aroeira LS, Aguilera A, Sanchez-Tomero JA, Bajo, MA, del Peso G, Jimenez-Heffernan JA, Selgas R, Lopez-Cabrera M.** Epithelial to mesenchymal transition and peritoneal membrane failure in peritoneal dialysis patients: pathologic significance and potential therapeutic interventions. *J Am Soc Nephrol* 18: 2004-2013, 2007.
2. **Berthier CC, Zhang H, Schin M, Henger A, Nelson RG, Yee B, Boucherot A, Neusser MA, Cohen CD, Carter-Su C, Argetsinger LS, Rastaldi MP, Brosius FC, Kretzler, M.** Enhanced expression of Janus kinase-signal transducer and activator of transcription pathway members in human diabetic nephropathy. *Diabetes* 58(2):469–477, 2009.
3. **Burkart, JM.** Peritoneal dialysis should be considered as the first line of renal replacement therapy for most ESRD patients. *Blood Purif* 19 :179-184, 2001.
4. **Chaudhary K, Sangha H, Khanna R.** Peritoneal dialysis first: Rationale. *Clin J Am Soc Nephro* 6 : 447-456, 2011.
5. **Cho Y, Johnson DW, Vesey DA, Hawley CM, Pascoe EM, Clarke M, Topley N and on behalf of the balANZ Trial Investigators.** Dialysate interleukin-6 predicts increasing peritoneal solute transport rate in incident peritoneal dialysis patients. *BMC Nephrology* 15:8, 2014.
6. **Chuang JH, Tung LC, Lin Y.** Neural differentiation from embryonic stem cells in vitro: an overview of the signaling pathways. *World J Stem Cells* 7:437–447, 2015.
7. **Davies SJ, Phillips L, Naish PF, Russell GI.** Peritoneal glucose exposure and changes in membrane solute transport with time on peritoneal dialysis. *J Am Soc Nephrol* 12: 1046-1051, 2001.
8. **Fielding, CA, Jones, GW, McLoughlin, RM, McLeod, L, Hammond, VJ, Uceda, J , Williams, AS, Lambie, M, Foster, TL, Liao, CT, Rice, CM, Greenhill, CJ, Colmont, CS, Hams, E, Coles, B, Kift-Morgan, A, Newton, Z, Craig, KJ, Williams, JD, Williams, GT, Davies, SJ, Humphreys, IR, O'Donnell, VB, Taylor, PR, Jenkins, BJ, Topley, N, Jones, SA.** Interleukin-6 Signaling Drives Fibrosis in Unresolved Inflammation. *Immunity* 40:40-50, 2014.
9. **Greenhill, CJ, Rose-John, S, Lissilaa, R, Ferlin, W, Ernst, M, Hertzog, PJ, Mansell, A, and Jenkins, BJ.** IL-6 trans-signaling modulates TLR4- dependent inflammatory responses via STAT3. *J Immunol*. 186, 1199–1208, 2011.
10. **He L, Lou W, Ji L , Liang W, Zhou M, Xu G, Zhao L, Huang C, Li R, Wang H, Chen X, Sun S.** Serum response factor accelerates the high glucose-induced Epithelial-to-Mesenchymal Transition (EMT) via snail signaling in human peritoneal mesothelial cells. *PLOS ONE* 9(10):e108593, 2014.
11. **Hou Y , Wu M , Wei J , Ren Y , Du C , Wu H , Li Y , Shi Y.** CD36 is involved in high glucose-induced epithelial to mesenchymal transition in renal tubular epithelial cells. *Biochem Biophys Res Commun* 468 (1-2): 281-286, 2015.

12. **Kadoya H, Satoh M, Nagasu H, Sasaki T, Kashihara, N.** Deficiency of endothelial nitric oxide signaling pathway exacerbates peritoneal fibrosis in mice. *Clin Exp Nephrol* 19(4):567-75, 2015.
13. **Lambie M, Chess J , Donovan KL, Kim YL, Do JY, Lee HB, Noh H, Williams PF , Williams AJ, Davison S, Dorval M, Summers A, Williams JD, Bankart J, Davies SJ , Topley N.** Independent Effects of Systemic and Peritoneal Inflammation on Peritoneal Dialysis Survival. *J Am Soc Nephrol* 24:2071–2080, 2013.
14. **Lim CP, Phan TT, Lim IJ, Cao X.** Cytokine profiling and Stat3 phosphorylation in epithelial-mesenchymal interactions between keloid keratinocytes and fibroblasts. *J Invest Dermatol* 129(4):851–861, 2009.
15. **Liu J, Zeng L, Zhao Y, Zhu B, Ren W, Wu C.** Selenium suppresses lipopolysaccharide-induced fibrosis in peritoneal mesothelial cells through inhibition of epithelial-to-mesenchymal transition. *Biol Trace Elem Res* 161(2):202-9, 2014.
16. **Mujais S, Nolph K, Gokal R, Ram G, Peter B, John B, Gerald C, Yoshindo K, Hideki K, Stephen K, Raymond K, Bengt L, Dimitrios O, Bengt R, and Rafael S.** Evaluation and management of ultrafiltration problems in peritoneal dialysis. For the International Society for Peritoneal Dialysis Ad Hoc Committee on Ultrafiltration Management in Peritoneal Dialysis. *Perit Dial Int* 20 : S5-S21, 2000.
17. **O'Donoghue RJ, Knight DA, Richards CD, Prêle CM, Lau HL, Jarnicki AG.** Genetic partitioning of interleukin-6 signalling in mice dissociates Stat3 from Smad3-mediated lung fibrosis. *EMBO Mol Med* 4:939–51, 2012.
18. **Ogata H, Chinen T, Yoshida T, Kinjyo I, Takaesu G, Shiraishi H, Iida M, Kobayashi T, Yoshimura A.** Loss of SOCS3 in the liver promotes fibrosis by enhancing STAT3-mediated TGF-be- ta1 production. *Oncogene* 25(17):2520–2530, 2006.
19. **Oh KH, Jung JY, Yoon MO, Song A, Lee H, Ro H, Hwang YH, Kim DK, Margetts P, Ahn C.** Intra-peritoneal interleukin-6 system is a potent determinant of the baseline peritoneal solute transport in incident peritoneal dialysis patients. *Nephrol Dial Transplant* 25(5):1639–1646, 2010.

20. **Pecoits R, Carvalho MJ, Stenvinkel P, Lindhom B, Heimburger O.** Systemic and intraperitoneal interleukin-6 system during the first year of peritoneal dialysis. *Perit Dial Int* 26(1): 53-63, 2006.
21. **Pecoits-Filho R, Barany P, Lindholm B, Heimburger O, Stenvinkel P.** Interleukin-6 is an independent predictor of mortality in patients starting dialysis treatment. *Nephrol Dial Transplant* 17(9): 1684-1688, 2002.
22. **Pedroza M, Schneider DJ, Karmouty-Quintana H, Coote J, Shaw S, Corrigan R, Molina JG, Alcorn, JL, Galas D, Gelinas R, Blackburn MR.** Interleukin-6 contributes to inflammation and remodeling in a model of adenosine mediated lung injury. *PLOS ONE* 6:e22667, 2011.
23. **Raible DJ, Frey LC, Del Angel YC, Carlsen J, Hund D, Russek SJ, Smith B, Brooks-Kayal AR.** JAK/STAT pathway regulation of GABAA receptor expression

after differing severities of experimental TBI. *Experimental Neurology* 271:445–456, 2015.

24. **Rumpsfeld M, McDonald SP, Johnson DW.** Higher peritoneal transport status is associated with higher mortality and technique failure in the Australian and New Zealand peritoneal dialysis patient populations. *J Am Soc Nephrol* 17(1):271–278, 2006.
25. **Samavati L, Rastogi R, Du W, Huttemann M, Fite A, Franchi L.** STAT3 tyrosine phosphorylation is critical for interleukin 1 beta and interleukin-6 production in response to lipopolysaccharide and live bacteria. *Mol Immunol* 46(8–9):1867–1877, 2009.
26. **Sei Y, Mizuno M, Suzuki Y, Imai M, Higashide K, Harris CL, Sakata F, Iguchi D , Fujiwara M, Kodera Y, Maruyama S, Matsuo S, Ito Y.** Expression of membrane complement regulators, CD46, CD55 and CD59, in mesothelial cells of patients on peritoneal dialysis therapy. *Molecular Immunology* 65:302-309, 2015.
27. **Suji K, Joung-Woo H, Kye WP.** B cell translocation gene 2 (Btg2) is regulated by Stat3 signaling and inhibits adipocyte differentiation. *Mol Cell Biochem* 413:145–153, 2016.
28. **Wang G, Wang JJ, Chen XL, Du SM, Li DS, Pei ZJ, Lan H, Wu LB.** The JAK2/STAT3 and mitochondrial pathways are essential for quercetin nanoliposome-induced C6 glioma cell death. Cell Death Dis 4:e746, 2013.
29. **Wang X, Shaw S, Amiri F, Eaton DC, Marrero MB.** Inhibition of the Jak/STAT signaling pathway prevents the high glucose-induced increase in tgf-beta and fibronectin synthesis in mesangial cells. *Diabetes* 51(12):3505–3509, 2002.
30. **Watanabe S, Mu W, Kahn A, Jing N, Li JH, Lan HY, Nakagawa T, Ohashi R, Johnson RJ.** Role of JAK/STAT pathway in IL-6-induced activation of vascular smooth muscle cells. *Am J Nephrol* 24(4):387–392, 2004.
31. **Weber CE, Li NY, Wai PY, Kuo PC.** Epithelial-mesenchymal transition, tgf-beta, and osteopontin in wound healing and tissue remodeling after injury. *J Burn Care Res* 33: 311-318, 2012.
32. **Xiao J, Gao HH Jin YF, Zhao ZH, Guo J, Liu ZS, Zhao ZZ.** The abnormal expressions of tristetraprolin and the VEGF family in uraemic rats with peritoneal dialysis. *Mol Cell Biochem* 392:229-238, 2014.
33. **Yuefei X, Nainin Y, Qingxian Z, Yiping W, Songtao Y, and Zhanxiao L.** Pentraxin 3 Inhibits Acute Renal Injury-Induced Interstitial Fibrosis Through Suppression of IL-6/Stat3 Pathway. *Inflammation* 37(5):1895-1901, 2014.
34. **Zeisberg M, Neilson EG.** Biomarkers for epithelial-mesenchymal transitions. *J Clin Invest* 119: 1429-1437, 2009.

482

Figure Legends:

Figure 1. Effect of IL-6 on HPMC morphology and viability

HPMCs were incubated at 37°C in a 5% CO2 atmosphere in DMEM medium without FBS. (A) HPMC morphology, (I) without treatment, (II) treated with 30 ng/mL IL-6, (III) with 50 ng/mL IL-6, and (IV) with 100 ng/mL IL-6 for 5 days. Magnification, ×200.

Normal HPMCs showed a cobblestone-like appearance(I), and its morphology had no obvious changes when cells were treated with 30 ng/mL IL-6. HPMCs which were treated with increased concentration IL-6 displayed a fibroblast-like morphology (III and IV). N = 6 per group.

(B) HPMC viability, without treatment vs. treated with 50 ng/mL IL-6 for 24, 48 and 72 hours; Absorbance value at 490 nm.

Cell viability was increased by 50 ng/mL IL-6. Compared with the same time, the values of the experimental groups were higher than that of no treatment group. * Statistical difference ($p < 0.05$). N = 6 per group. Data are means ± SE.

Figure 2. Protein and mRNA expressions of E-cadherin, α-SMA, and VEGF in IL-6 cultured HPMCs at 24 hours

Western blotting analysis for protein expression: (A), raw photo and (B), densitometry analysis; β-actin as the housekeeping gene to normalize expression level. Real-time fluorescence quantitative PCR for mRNA expression: (C), for E-cadherin, (D) for α-SMA and (E) for VEGF; GAPDH as the housekeeping gene to normalize expression level.

The protein and mRNA expression of α-SMA and VEGF increased significantly following exposure to IL-6, peaking at 100 ng/mL. On the contrary, the expression of E-cadherin was downregulated by IL-6. *Statistical significant ($p < 0.05$) vs. no treatment. N = 6 per group. Data are means ± SE.

Figure 3. Protein and mRNA expressions of E-cadherin, α-SMA, and VEGF in 50 ng/ml IL-6 cultured HPMCs at 24, 48 and 72 hours

Western blotting analysis for protein expression: (A), raw photo and (B), densitometry analysis; β-actin as the housekeeping gene to normalize expression level. Real-time fluorescence quantitative PCR for mRNA expression: (C), for E-cadherin, (D) for α-SMA and (E) for VEGF; GAPDH as the housekeeping gene to normalize expression level.

The expression of α-SMA and VEGF increased significantly following exposure to IL-6, peaking at 72 h respectively. On the contrary, the expression of E-cadherin decreased as the stimulus time of IL-6 extends. *Statistical significant ($p < 0.05$) vs. no treatment. N = 6 per group. Data are means ± SE.

Figure 4. Protein expressions of JAK2 and STAT3 in IL-6 cultured HPMCs at 24, 48 and 72 hours

Western blotting analysis for protein expression: (A,C), raw photo and (B,D), densitometry analysis; P-JAK2, phosphorylated JAK2; P-STAT3, phosphorylated STAT3; β-actin as the housekeeping gene to normalize expression level.

(A,B) The relative protein expression of active JAK2/STAT3 increased significantly following exposure to IL-6, peaking at 100 ng/mL, respectively. * Statistical significant ($p < 0.05$) vs. no treatment. N = 9 per group. Data are means ± SE.

(C,D) The relative protein expression of active JAK2/STAT3 increased significantly following exposure to IL-6, peaking at 72 h respectively. * Statistical significant ($p < 0.05$) vs. no treatment. N = 9 per group. Data are means ± SE.

Figure 5. The effect of WP1066 on the expression of P-STAT3/STAT3 at 24 hours

Western blotting analysis for protein expression: (A), raw photo and (B), densitometry analysis; β-actin as the housekeeping gene to normalize expression level. The relative protein expression of active STAT3 (phosphorylated/total) decreased significantly in exposure to 10 *μM* WP1066; * $p < 0.05$ (vs. no treatment). N = 12 per group. Data are means ± SE.

Figure 6. Phosphorylated and total protein expressions of JAK2 and STAT3 in HPMCs with IL-6 and WP1066 treatment at 24 hours

Western blotting analysis for protein expression: (A), raw photo and (B), densitometry analysis; (I) no treatment (without IL-6, without WP1066); (II) IL-6 (with IL-6, without WP1066); (III) IL-6+WP1066 group (with IL-6, with WP1066); (IV) WP1066 (without IL-6, with WP1066); β-actin as the housekeeping gene to normalize expression level.

The relative protein expression of active JAK2/STAT3 increased significantly following exposure to 100 ng/ml IL-6, * Statistical significant ($p < 0.05$) vs. no treatment. When adding to 10 *μM* WP1066, the activation of JAK2/STAT3 which was induced by IL-6 was prevented obviously. N = 12 per group. Data are means ± SE.

Figure 7. Protein expressions of E-cadherin, α-SMA and VEGF in HPMCs with IL-6 and WP1066 treatment at 24 hours

Western blotting analysis for protein expression: (A), raw photo and (B), densitometry analysis; β-actin as the housekeeping gene to normalize expression level. (I) no treatment (without IL-6, without WP1066); (II) IL-6 (with IL-6, without WP1066); (III) IL-6+WP1066 group (with IL-6, with WP1066); (IV) WP1066 (without IL-6, with WP1066). Real-time fluorescence quantitative PCR for mRNA expression: (C), for E-cadherin, (D) for α-SMA and (E) for VEGF; GAPDH as the housekeeping gene to normalize expression level.

The relative protein and mRNA expression of α-SMA and VEGF increased significantly following exposure to 100 ng/ml IL-6, which also decreased E-cadherin expression, * Statistical significant ($p < 0.05$) vs. no treatment. When adding to 10 *μM* WP1066, the expression changes of α-SMA, VEGF and E-cadherin prevented obviously. N = 9 per group. Data are means ± SE.

Figure 8. Effect of WP1066 on cell morphology and viability in IL-6 treated HPMCs

HPMCs were incubated at 37°C in a 5% CO2 atmosphere in DMEM medium without FBS. (A) HPMC morphology, cultured for 5 days; (I) no treatment (without IL-6, without WP1066); (II) IL-6 (with IL-6, without WP1066); (III) IL-6+WP1066 group (with IL-6, with WP1066); (IV) WP1066 (without IL-6, with WP1066). Magnification, ×200. (B) HPMC viability, cultured for 0 and 24 hours; Absorbance value at 490 nm.

IL-6 induced morphologic change of HPMCs and an increased cell proliferation. When adding WP1066, the effect of IL-6 was prevented. Compared with no treatment, The morphology and viability of HPMCs had no changes. * Statistical difference ($p < 0.05$) between with and without treatment. N = 6 per group. Data are means ± SE.

Table 1. Patient recruitment criteria

Eligibility criteria	Exclusion criteria
PD >3 months	Presence of systemic inflammatory disease, peritonitis or fluid overload 3 months;
≥18 years old	Malignant tumor;
blood pressure <140/90mmHg	Taking glucocorticoid or immunosuppressive agents during the past 1 year;
Hemoglobin A1C(HbA1C) <9%	Acute cardio cerebrovascular events that occurred in past 3 months;
PD solution: Dianeal Baxter company	Multiple organ dysfunction syndrome; Systemic inflammatory response syndrome.

Inclusion, meet all eligibility criteria; Exclusion, meet any exclusion criteria. PD, peritoneal dialysis.

Table 2. Sequences of mRNA

Gene Symbol	Forward Primer(5'-3')	Reverse Primer(5'-3')
E-cadherin	CTCTTCTCCGCCTCCTTCTT	TGATTCTGCTGCTCTTGCTG
α-SMA	AAGATGACCCAGATCATGTT	TCATAGATGGGGACATTGT
VEGF	ATGACGAGGGCCTGGAGTGT	GGGATTTCTTGGGCTTTCGTTT
GAPDH	CCTCAAGATCATCAGCAAT	CCATCCACAGTCTTCTGGGT

Table 3. Patient characteristics and IL-6 levels

Characteristics	PD (n=20)	UFF (n=20)	*p* value
Clinical-demographic			
Age, years	43 ±14	41±15	0.6
Male	11(55%)	11(55%)	1.0
BMI	23.6±3.2	22.5±2.5	0.2
BSA, m^2	1.6±0.5	1.6±0.5	0.9
PD duration, months	24.85(10-40)	27.20(12-37)	0.4
Laboratory measures			
Serum albumin, g/l	30.1±3.5	30.2±3.2	0.9
Hs-CRP, mg/l	4.8±2.8	5.0±2.8	0.8
Hemoglobin, g/l	89.6±16.3	88.1±8.9	0.7
PD adequacy			
Total Kt/v urea	1.8±0.2	1.6±0.2	<0.01
Peritoneal Kt/v urea	1.6±0.2	1.4±0.1	0.04
Renal Kt/v urea	0.2±0.1	0.1±0.1	0.02
Urine output, ml/24h	713(200-1250)	400(50-700)	<0.01
24 h Ultrafiltration, ml/24h	628(200-1300)	100(-300-310)	<0.01
Dialysate glucose exposure, g/day	132.2±25.6	142.6±30.5	0.2
peritoneal equilibration test (PET)			
4 h Ultrafiltration, ml/4h	550(400-750)	30(-200-300)	<0.01
dialysate/ plasma creatinine (D/PCr)	0.6±0.2	0.8±0.1	<0.01
IL-6 level			
Plasma level (pg/mL)	20.7±5.0	69.3±16.5	<0.01
Dialysate level (IL-6 Appearance rate, pg/min)	96.1±20.5	448.0±51.6	<0.01

PD, patients under scheduled peritoneal dialysis care; UFF, patients occurred peritoneal ultrafiltration failure.

Table 4. Correlation test between IL-6AR level in dialysate with selected patient characteristics (all patients n=40)

Variable	r	*p* value
BSA	0.09	0.59
PD duration	0.39	0.01
Hs-CRP	0.27	0.09
Total Kt/v urea	-0.48	<0.01
Peritoneal Kt/v urea	-0.33	0.04
Urine output	-0.44	<0.01
24 hour Ultrafiltration	-0.81	<0.01
4 h Ultrafiltration	-0.78	<0.01
D/PCr	0.63	<0.01

PD, patients under scheduled peritoneal dialysis care; UFF, patients occurred peritoneal ultrafiltration failure; r, correlation coefficient.

Figure 1.

A

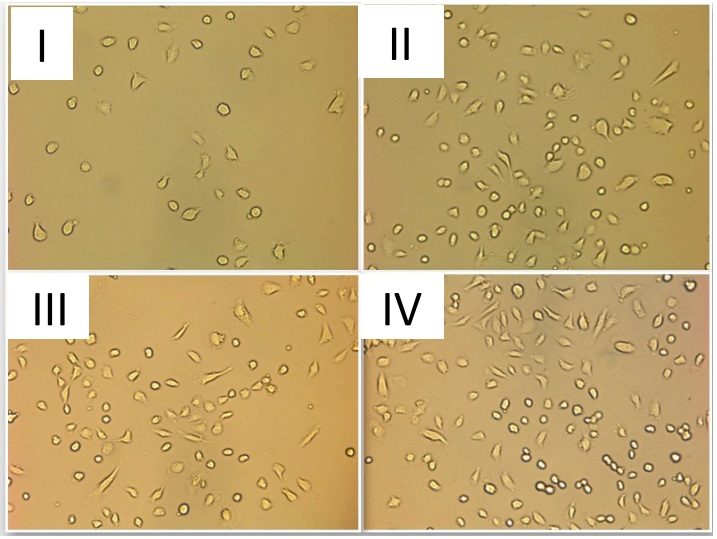
I
II
III
IV

B

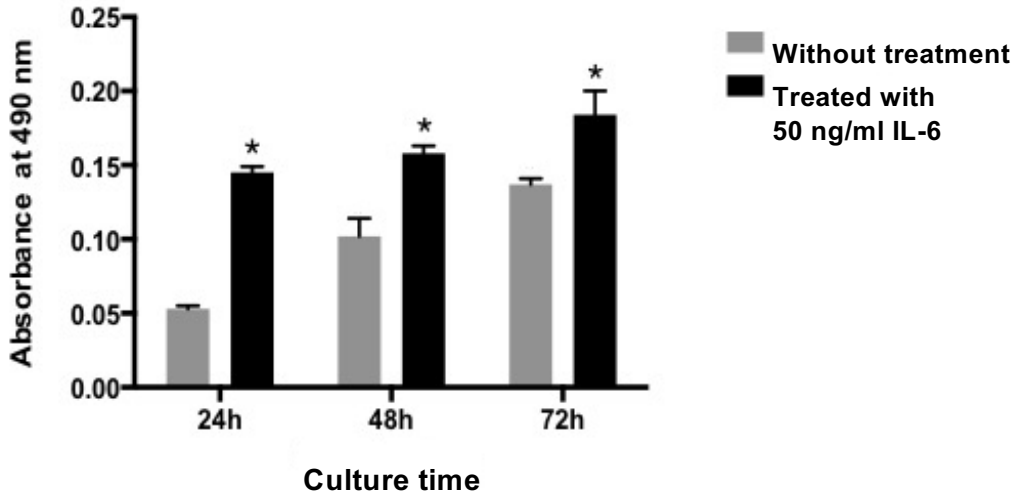
Absorbance at 490 nm
0.25
0.20
0.15
0.10
0.05
0.00
*
*
*
24h
48h
72h
Culture time
Without treatment
Treated with
50 ng/ml IL-6

Figure 2.

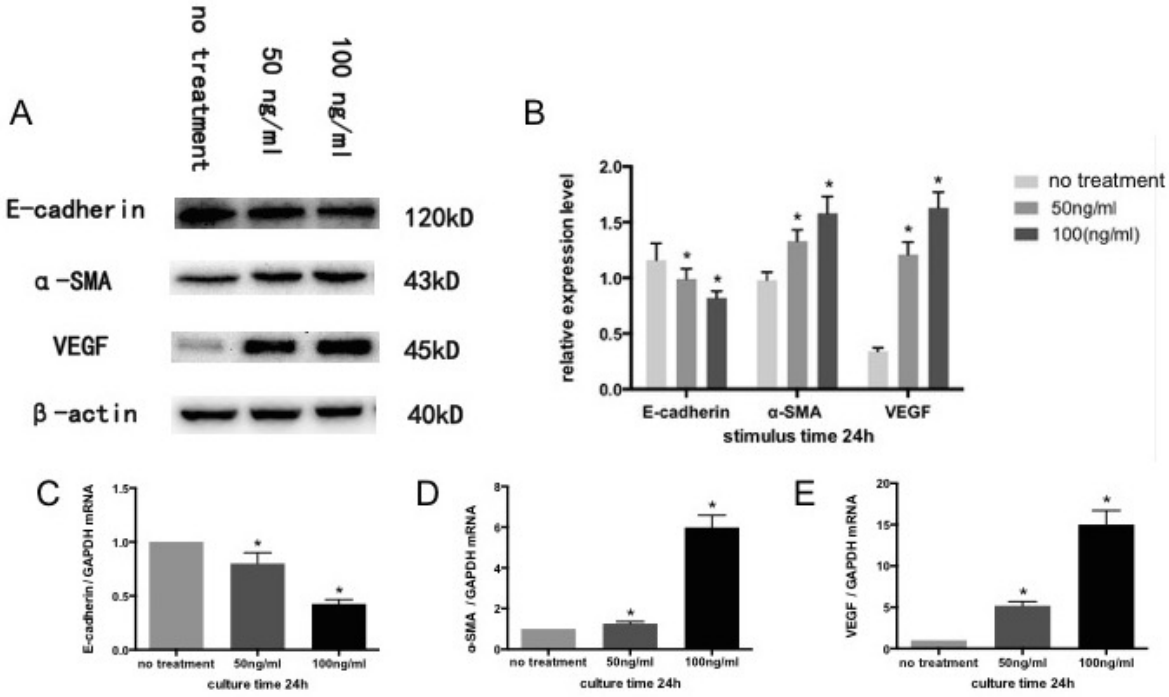
A
no treatment
50 ng/ml
100 ng/ml
E-cadherin
α-SMA
VEGF
β-actin
120kD
43kD
45kD
40kD
B
relative expression level
2.0
1.5
1.0
0.5
0.0
E-cadherin
α-SMA
VEGF
stimulus time 24h
no treatment
50ng/ml
100(ng/ml)
C
E-cadherin / GAPDH mRNA
no treatment
50ng/ml
100ng/ml
culture time 24h
D
α-SMA / GAPDH mRNA
no treatment
50ng/ml
100ng/ml
culture time 24h
E
VEGF / GAPDH mRNA
no treatment
50ng/ml
100ng/ml
culture time 24h

Figure 3.

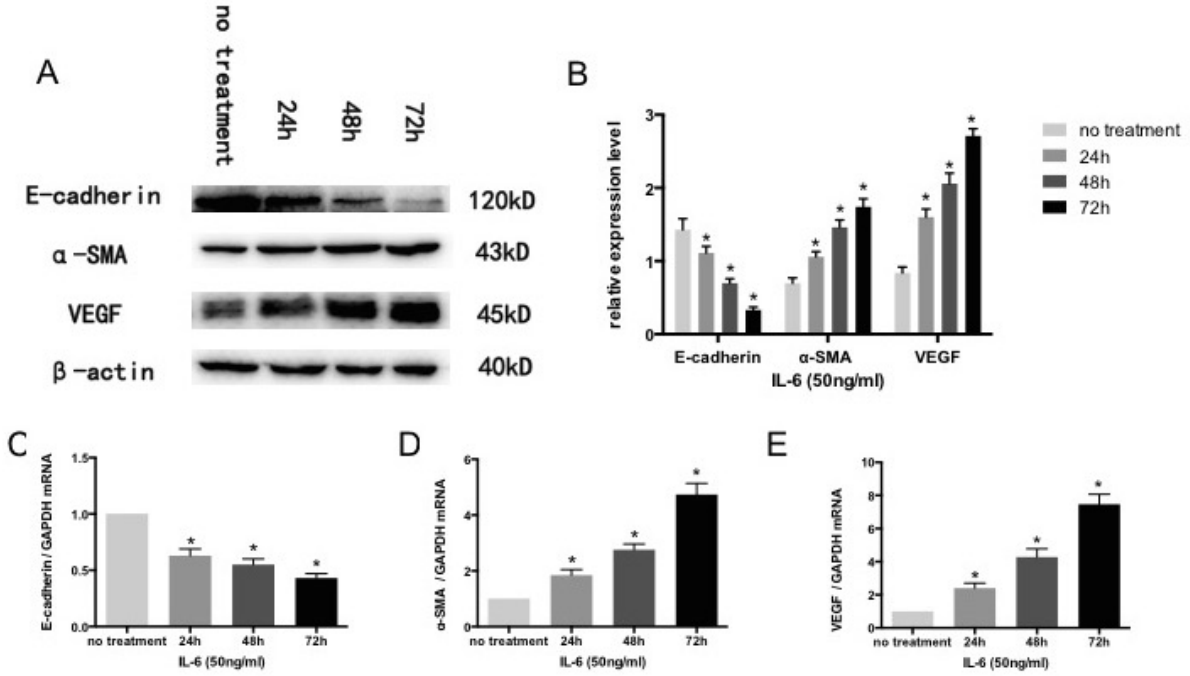
A
no treatment
24h
48h
72h
E-cadherin
α-SMA
VEGF
β-actin
120kD
43kD
45kD
40kD
B
relative expression level
no treatment
24h
48h
72h
E-cadherin
α-SMA
VEGF
IL-6 (50ng/ml)
C
E-cadherin / GAPDH mRNA
no treatment
24h
48h
72h
IL-6 (50ng/ml)
D
α-SMA / GAPDH mRNA
no treatment
24h
48h
72h
IL-6 (50ng/ml)
E
VEGF / GAPDH mRNA
no treatment
24h
48h
72h
IL-6 (50ng/ml)

Figure 4.

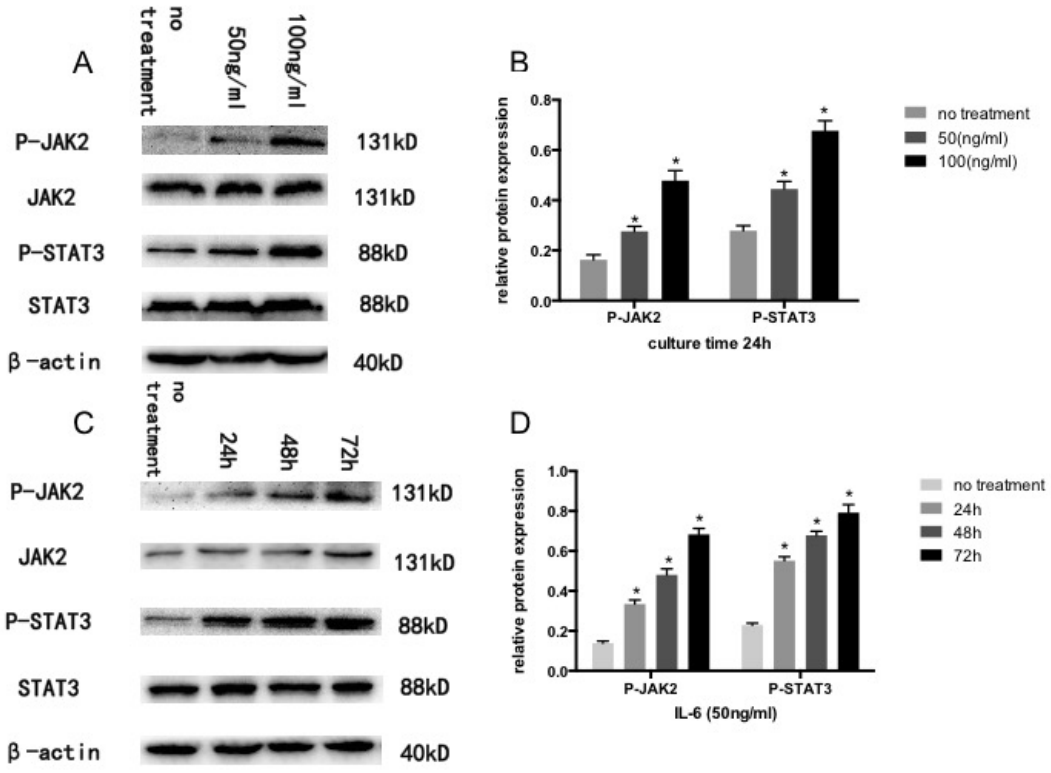
A
no treatment
50ng/ml
100ng/ml
P-JAK2
JAK2
P-STAT3
STAT3
β-actin
131kD
131kD
88kD
88kD
40kD
B
relative protein expression
0.0
0.2
0.4
0.6
0.8
P-JAK2
P-STAT3
culture time 24h
no treatment
50(ng/ml)
100(ng/ml)
C
no treatment
24h
48h
72h
P-JAK2
JAK2
P-STAT3
STAT3
β-actin
131kD
131kD
88kD
88kD
40kD
D
relative protein expression
0.0
0.2
0.4
0.6
0.8
1.0
P-JAK2
P-STAT3
IL-6 (50ng/ml)
no treatment
24h
48h
72h

Figure 5.

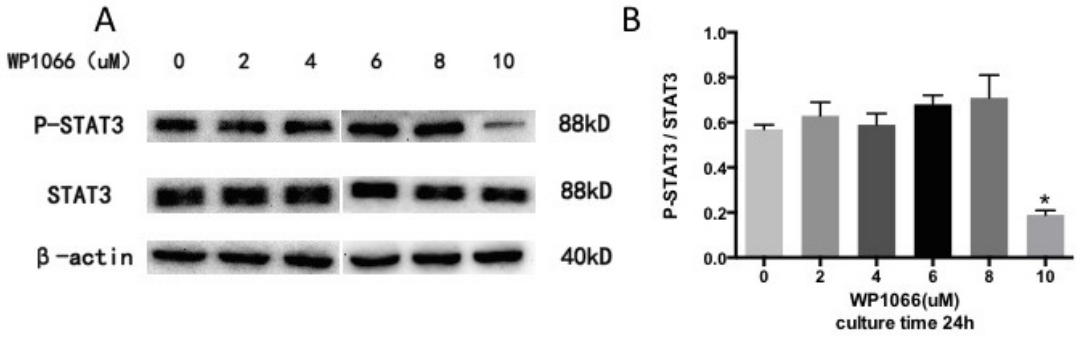
A
WP1066 (uM) 0 2 4 6 8 10
P-STAT3
STAT3
β-actin
88kD
88kD
40kD
B
P-STAT3 / STAT3
1.0
0.8
0.6
0.4
0.2
0.0
0 2 4 6 8 10
WP1066(uM)
culture time 24h
*

Figure 6.

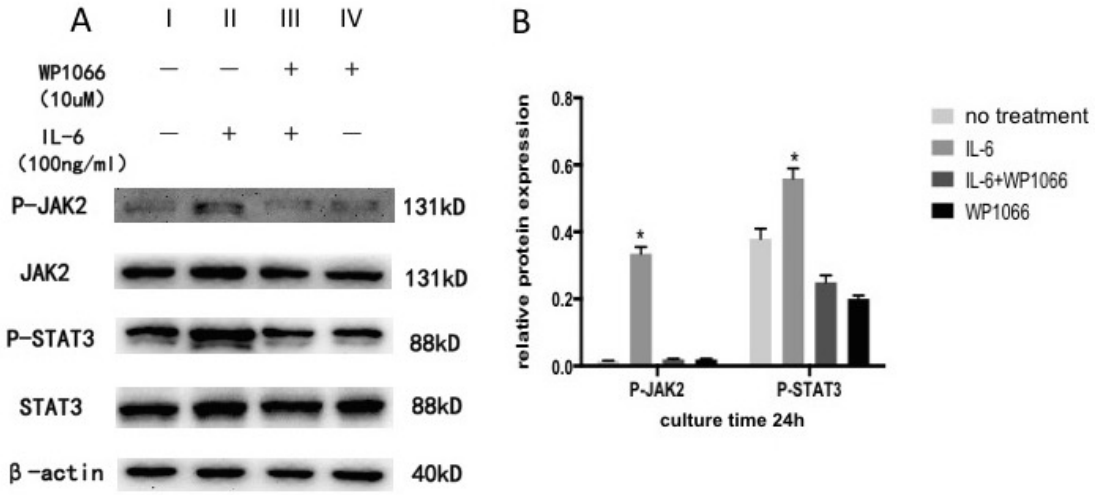
A
I
II
III
IV
WP1066 (10uM)
IL-6 (100ng/ml)
P-JAK2
131kD
JAK2
131kD
P-STAT3
88kD
STAT3
88kD
β-actin
40kD
B
relative protein expression
0.8
0.6
0.4
0.2
0.0
P-JAK2
P-STAT3
culture time 24h
no treatment
IL-6
IL-6+WP1066
WP1066

Figure 7.

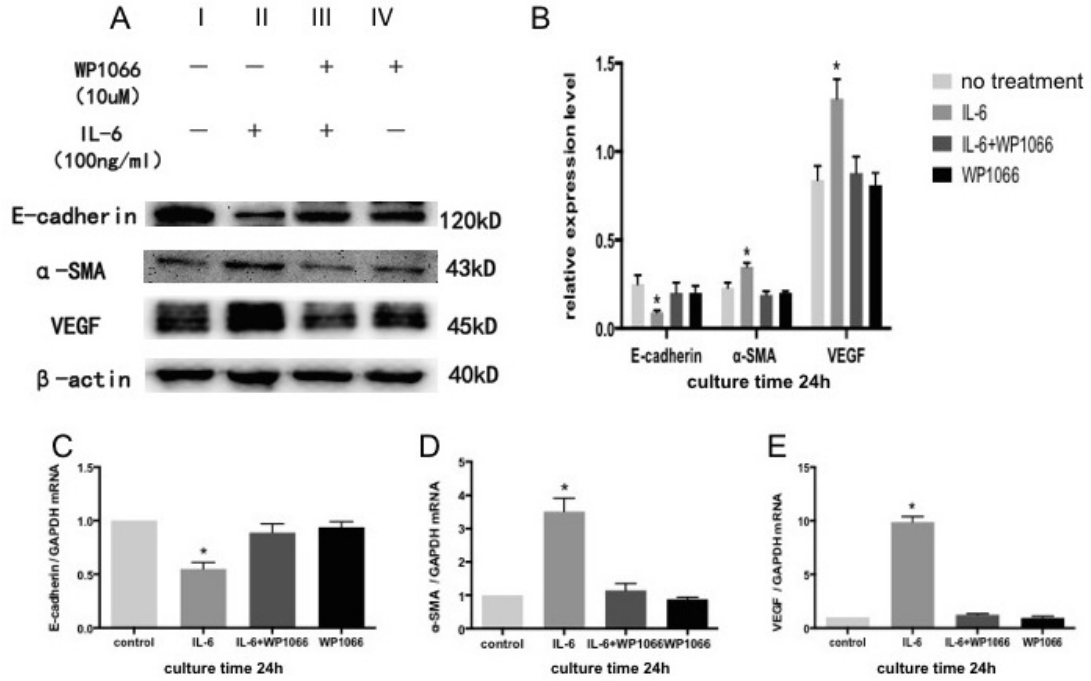
A
I
II
III
IV
WP1066 (10uM)
IL-6 (100ng/ml)
E-cadherin
α-SMA
VEGF
β-actin
120kD
43kD
45kD
40kD
B
relative expression level
no treatment
IL-6
IL-6+WP1066
WP1066
E-cadherin
α-SMA
VEGF
culture time 24h
C
E-cadherin/GAPDH mRNA
control
IL-6
IL-6+WP1066
WP1066
culture time 24h
D
α-SMA /GAPDH mRNA
control
IL-6
IL-6+WP1066
WP1066
culture time 24h
E
VEGF /GAPDH mRNA
control
IL-6
IL-6+WP1066
WP1066
culture time 24h

Figure 8.

A

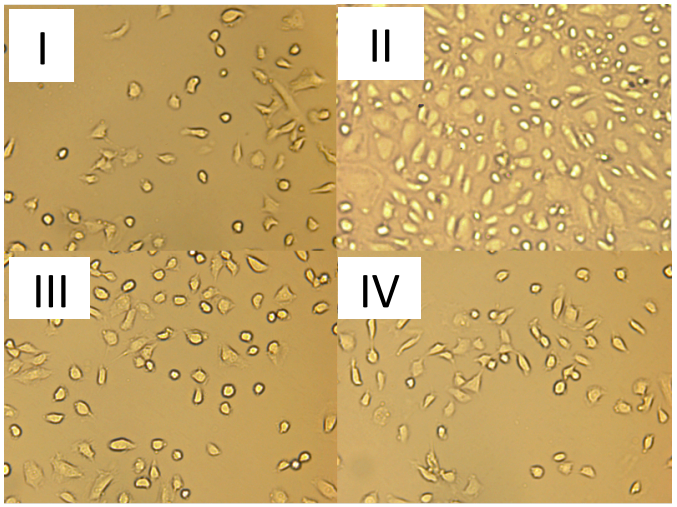
I
II
III
IV

B

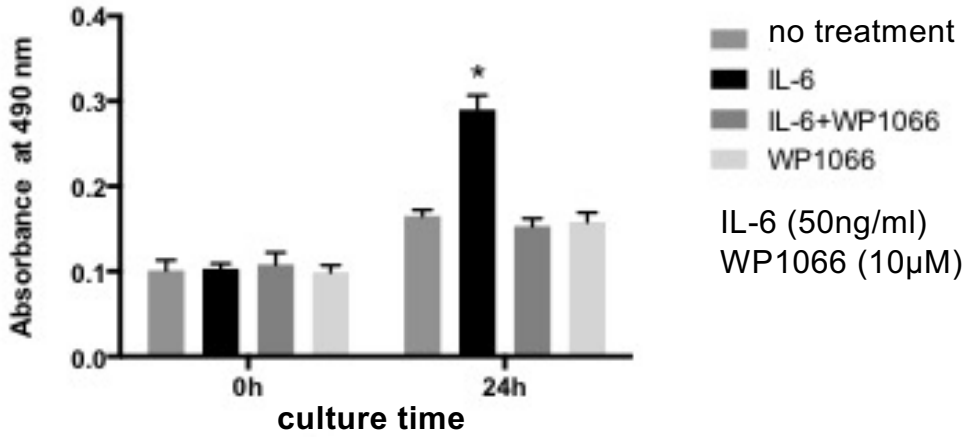
Absorbance at 490 nm
0.4
0.3
0.2
0.1
0.0
*
0h
24h
culture time
no treatment
IL-6
IL-6+WP1066
WP1066
IL-6 (50ng/ml)
WP1066 (10μM)